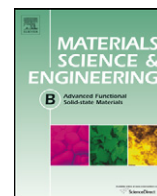




Contents lists available at ScienceDirect

Materials Science and Engineering B

journal homepage: www.elsevier.com/locate/mseb

Vacancies and E-centers in silicon as multi-symmetry defects

M.G. Ganchenkova^{a,*}, L.E. Oikkonen^a, V.A. Borodin^b, S. Nicolaysen^c, R.M. Nieminen^a^a Helsinki University of Technology, P.O. Box 1100, 02015 Espoo, Finland^b RRC Kurchatov Institute, 123182 Moscow, Russia^c Institute for Microsystem Technology, P.O. Box 2243, N-3103 Tonsberg, Norway

ARTICLE INFO

Article history:

Received 16 May 2008

Received in revised form 6 October 2008

Accepted 16 October 2008

Keywords:

Silicon

Vacancy

E-center

Calculations

ABSTRACT

In this paper, using first-principles calculations, we demonstrate that vacancies and E-centers (AsV, SbV) in silicon can co-exist in several metastable configurations with notably different relaxation patterns, which have very similar formation energies. Thus these vacancy-type defects can be considered as multi-symmetry defects in the sense that, at elevated temperatures, the probabilities to find vacancies in different stable configurations are comparable. From an experimental point of view, the co-existence of various symmetries can complicate the identification of the defect.

© 2008 Elsevier B.V. All rights reserved.

1. Introduction

Silicon is the most widely used semiconductor among those applied for microelectronics. Even after many years of active search for alternative materials, silicon still dominates the market and is incorporated in over 90% of electronic devices [1]. Along with its other advantages, such as good material availability and suitable band gap, one of silicon's major assets is the high sensitivity of its electrical properties to relatively small amounts of doping impurities such as boron (B), phosphorus (P), or arsenic (As).

Because the reliable control of microelectronic device material performance is impossible without a detailed knowledge of the properties of defects it contains, the research on defects in silicon is an active field of microelectronics-related materials science. This research field has been faced with a broad spectrum of experimental approaches, largely supported by numerical simulations using such atomistic computational techniques as first-principles calculations, molecular dynamics, and kinetic Monte-Carlo [2–9]. One might expect that everything worth knowing on defect properties in Si has already been discovered, but in reality our understanding of the defect properties and kinetics remains far from complete.

Indeed, defect parameters and properties have broad uncertainty ranges even for the most basic defects in Si, such as vacancies, small vacancy clusters and vacancy-donor pairs (E-centers). For instance, the estimates of the monovacancy formation energy by different experimental and computational techniques fluctuate by

more than 1 eV [2–7,10–16]. The same uncertainty is typical for defect migration energies [10–12,17,18].

From the experimental side, the scatter in the defect energy parameters is largely due to the difficulty of their direct determination. Very sophisticated measurements are used to obtain the data on the defect properties, and even then the extraction of defect parameters from the data remains largely interpretation dependent. For example, the most recent estimate of the vacancy formation energy, 3.15 eV, is derived [16] from a combination of the self-diffusion measurements of Shimizu et al. [19] and the neutral vacancy migration value deduced from [20,21]. To make things worse, the results of different techniques are often not compatible with each other. One of the reasons for this is the sensitivity of the defect formation energy to the Fermi level position in the crystal, so that the experimental results can vary depending on the sample doping level. Computational studies, on the other hand, are limited by the amount of computer resources required by the most reliable simulation techniques, which are often the only applicable ones. As a result, even for the simplest defect – monovacancy in silicon – numerical studies have been restricted for a long time only to the neutral charge state [4–7] and to small simulation cells and *k*-point sets [2,3,22,23].

Another issue that has been studied extensively without reaching a final agreement is the elastic relaxation pattern of vacancies and E-centers. The first model of anisotropic distortion for the silicon vacancy has been proposed by Watkins in Ref. [24]. It has been demonstrated that the relaxation pattern of the four silicon atoms constituting the first nearest-neighbor shell of a vacant lattice site should vary as a function of the defect charge. According to this model, the distortion for V^+ and V^0 is tetragonal, resulting in D_{2d}

* Corresponding author. Tel.: +358 468103138; fax: +358 9 4513116.

E-mail address: mgc@fyslab.hut.fi (M.G. Ganchenkova).

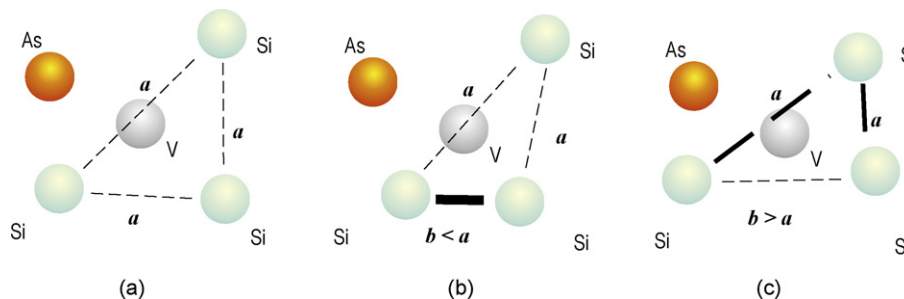


Fig. 1. Schematic representation of the vacancy nearest-neighbor distortion modes: breathing (a), pairing (b) or resonant (c).

symmetry of the relaxation pattern, whereas for V^- and V^{2-} , the symmetry is further lowered down to C_{2v} . Later on, it has been demonstrated [25] that purely symmetry-based arguments are not sufficient to guarantee either the predicted relaxation pattern, or its energetic proficiency. Accounting for the effects related to the elastic relaxation around the defect is at least equally important. For example, too strong elastic distortions around the vacancy in silicon were demonstrated to forbid the V^+ charge state [25,26]. More recent *ab initio* calculations [2–4,22,23,27] confirm a noticeable inward relaxation of the vacancy environment accompanied with the symmetry lowering. However, the predicted vacancy symmetries vary from one calculation to another.

Similar uncertainties are met where the relaxation pattern of E-centers in silicon is concerned. Three main modes of vacancy environment relaxation in E-center have been suggested by now, namely—breathing, pairing and resonant distortion patterns (see Fig. 1). The breathing distortion keeps equal bond lengths between the silicon atoms nearest to a vacant site. In contrast, resonant and pairing distortions break the initial symmetry. In pairing mode, weak covalent bonds are formed between the vacancy neighbours in such a way that one of the three bonds is noticeably shorter than the other two. In resonant bonding, no bond is formed between two vacancy neighbours and the corresponding interatomic distance turns out to be longer than between the bound atoms. Pairing is claimed to be observed in the case of a neutral E-center in EPR studies [14,28], whereas stress measurements [29] indicate resonant bonding in the negatively charged state. Density-functional theory (DFT) cluster calculations for AsV by Ögüt and Chelikowsky [30] are in favour of these interpretations. However, for the PV complex the resonant bonding configuration has been proposed to be the ground state in all possible charge states [31].

In this paper, using first-principles calculations, we demonstrate that vacancies and E-centers (AsV, SbV) in silicon do not exhibit one dominant relaxation pattern. Instead, these vacancy-type defects can be considered as multi-symmetry defects since, at each charge state, there exist several metastable defect configurations with notably different relaxation patterns, but with very similar formation energies.

2. Computational details

The vacancy configurations with different relaxation patterns, even if exist, correspond to some local total energy minima and it is not easy to scan all the desired symmetries starting from completely arbitrary initial configurations, as it has been done, e.g. in [32]. Hence, we have adopted a “predefined initial symmetry” strategy, where the initial shifts of the atoms in the 1NN shells of the defects were constrained to different point symmetry groups. The considered initial symmetries included T_d , D_{2d} , C_{2v} , and C_{3v} , as well as the ‘split’ configuration of D_{3d} symmetry. However, no further symmetry restrictions were imposed during the atomic relaxation

to the nearest elastically stable configurations. The approach is very similar in its spirit to that adopted in [32], where, however, only T_d , D_{2d} and C_{3v} starting patterns were considered and somewhat different calculation conditions were employed.

The results reported here have been obtained using the spin-polarized generalized gradient approximation (GGA) [33] for the exchange–correlation description as implemented in the DFT-based program VASP [34,35]. GGA-s is usually assumed to better reproduce the vacancy properties than the other broadly used local density approximation (LDA or, where spin polarization is treated explicitly, LSDA) [36]. In fact, we have checked that the use of LSDA does not affect the elastic stability of any considered configuration, even though the relaxation patterns are slightly different. Therefore, we focus on discussing the GGA results. The ultrasoft Vanderbilt-type pseudopotential [37] was used for all calculations. We used a supercell of 216 atoms, with the silicon lattice parameter of 5.46 Å. The Brillouin zone (BZ) sampling was done using the $(2 \times 2 \times 2)$ k -point mesh of Monkhorst and Pack [38] and the cutoff energy was 250 eV. A relaxation run was terminated when the Hellmann–Feynman forces on all atoms fell below 0.01 eV/Å, or the total energy variation within one electronic relaxation step fell below 10^{-4} eV.

3. Results and discussion

The monovacancy in silicon was studied starting from five above-mentioned symmetries in five charge states, as listed in Table 1. In order to permit comparison of different configurations from the energy proficiency point of view, Table 1 presents for different stable vacancy configurations only the formation energy excess over the lowest formation energy in each charge state, while the lowest formation energies themselves are given in Table 2. As can be immediately seen, starting from V^+ , the monovacancy can exist in several metastable configurations with different symmetries. The maximum difference in energy with the lowest energy configuration is only 0.2 eV, which makes all configurations feasible.

In full agreement with all earlier studies, the vacancy in charge state $2+$ is uniquely characterized by T_d symmetry of its relaxation pattern. In the V^+ charge state, the same ground-state energy was

Table 1
Formation energies with respect to the lowest formation energy of each charge state.

Vacancy symmetry	V^{2+}	V^+	V^0	V^-	V^{2-}
T_d	0.00	–	–	0.07	0.20
$D_{2d}(A)$	–	0.00	0.00	0.01	0.19
$D_{2d}(B)$	–	0.00	0.17	0.06	0.10
C_{2v}	–	–	0.00	0.00	0.20
C_{3v}	–	–	0.18	–	–
C_{2h}	–	–	–	0.00	–
D_{3d} (‘split’)	–	0.20	0.20	0.04	0.00

Table 2

Formation energies and symmetries of the most energetically favorable configurations at each charge state. The obtained results are compared to other *ab initio* calculations for the same supercell size (216 lattice sites) and to experimental data.

Charge	Formation energy (eV)				Symmetry			
	This work	Ref. [2] LSDA	Ref. [32] GGA	Exp. [9–15]	This work	Ref. [2] LSDA	Ref. [32] GGA	Exp.
+2	3.48	3.01	3.28		T_d	T_d	T_d	T_d [18]
+1	3.61	3.20	3.53		$\sim D_{2d}$	$\sim D_{2d}$	D_{2d}	D_{2d} [18]
0	3.67	3.31	3.66	2.1–3.6	D_{2d}	$\sim D_{2d}$	D_{2d}	D_{2d} [18]
−1	4.04	3.88	4.17		C_{2v}	$\sim D_{3d}$	C_{2v}	C_{2v} [18]
−2	4.40	4.29	4.51		D_{3d} (split)	$\sim D_{3d}$	D_{3d}	C_{2v} [18] D_{3d} [39]

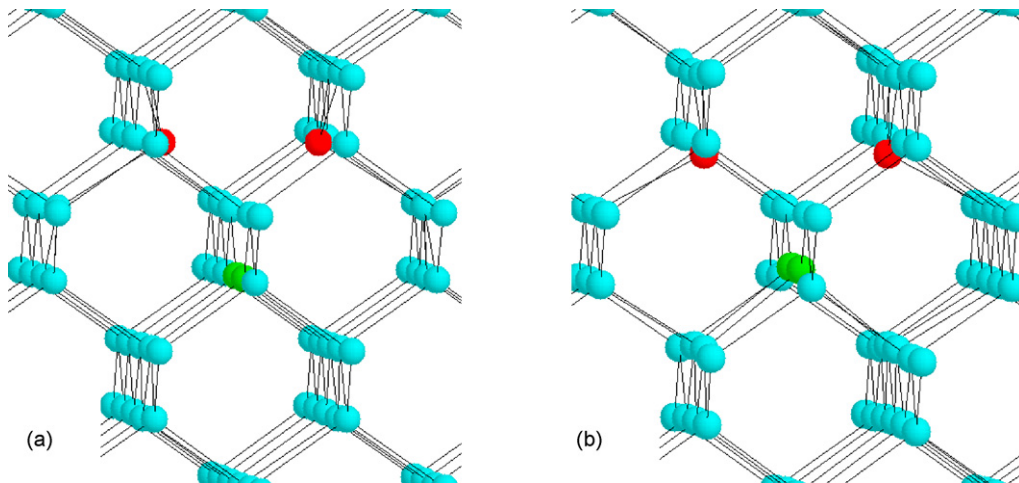


Fig. 2. The local atomic configurations in the vicinity of vacancies with relaxation patterns: (a) $D_{2d}(A)$ and (b) $D_{2d}(B)$. Vacancy neighbors connected by “pairing” 2NN bonds are drawn in red and green. Note also the completely different relaxation pattern of the 2NN shell of the vacancy. (For interpretation of the references to color in this figure legend, the reader is referred to the web version of the article.)

found for two configurations that have the same symmetry (D_{2d}), but different relaxation patterns (see Fig. 2). However, the degree of pairing distortion is very low (the distances between the vacancy first-nearest neighbors (1NN) vary within 0.01–0.02 Å) and from the practical point of view both these configurations are indistinguishable from T_d . In addition, the split configuration remained unaltered by the relaxation, though its energy is larger than that of the ground state. We cannot also exclude the existence of D_{2d} configurations with meaningful differences between the vacancy 1NN atom separations, as reported (especially for larger supercell sizes) in [32], but we failed to create such an initial configuration that would relax into them.

For neutral vacancies, our calculations predict the stability of five configurations, two of which have the same symmetry (D_{2d}), but different relaxation patterns (see Fig. 2). The lowest energy configurations are $D_{2d}(A)$ and C_{2v} , with a negligible difference in their formation energies. The remaining stable configurations have formation energies exceeding that of the ground state by ~ 0.2 eV. In some cases, the difference in energy can be attributed to differences in their spin states.

The addition of one more electron to the neutral vacancy results in the appearance of just another relaxation pattern, with C_{2h} symmetry. In terms of the energy proficiency, it is the next to the ground state, which in the case of V^- is unique and corresponds to C_{2v} . The latter conclusion agrees with the predictions of the well-known EPR and ENDOR experiments [18,26] and recent GGA calculations [32], but differs from the earlier *ab initio* calculations that were in favor of the split configuration [2], which in our case is only the fourth in the list. Neither did we observe a spontaneous transition from T_d to a split configuration. Finally, a non-trivial vacancy configuration, the split one, is found to be the ground state for the doubly negatively

charged vacancies, in agreement with Refs. [2,32,38]. The spread in the vacancy formation energies for different stable configurations falls within only 0.2 eV.

Comparing relaxation patterns with similar energies, one can see that they look out too different to be ascribed to the relaxation procedure problems. However, the co-existence of several vacancy symmetries is often attributed to uncertainties in finding the ground state atomic configuration [2]. In order to be on the safe side, it would be desirable to explicitly determine the energy tran-

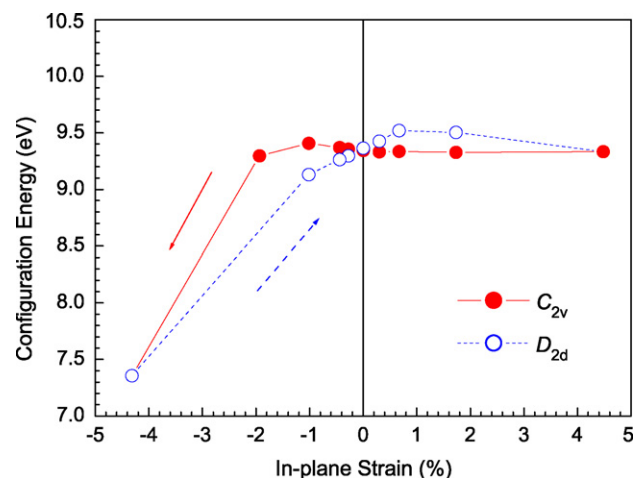


Fig. 3. The variation of monovacancy configuration energy during the plane strain cycling. Calculated values are shown with full and hollow circles, connected by straight lines to guide the eye. The strain cycling direction is indicated by arrows.

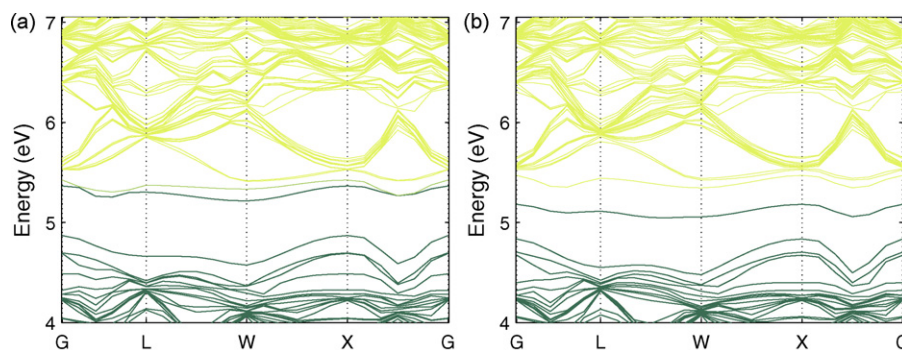


Fig. 4. Band structure of AsV in silicon for RB (left) and PB (right) relaxation modes.

sition barriers between different configurations. Unfortunately, in order to quantify transitions between defect symmetries, one has to follow the collective motion of atoms in at least the first two nearest neighbour shells from the defects. The straightforward search for the saddle point positions by variation of the multiple degrees of freedom for all the atoms involved is a too ambitious task for our available computational facilities. Therefore, we have tried to demonstrate the presence of the barriers indirectly by investigating the reaction of vacancy symmetries to anisotropic elastic strain cycling. In the simulations exemplified in Fig. 3, the simulation cell with a vacancy in initial D_{2d} configuration was strained in compression in discrete strain steps until a spontaneous transformation into a new symmetry (here C_{2v}) took place. After that, the strain direction was reversed and the strain was increased until the reverse transformation took place. It has been found that the strain direction reversal switches C_{2v} back to D_{2d} only when sufficiently high tensile strain is reached. It is hard to explain the observed hysteresis of the vacancy configurational energy, as shown in Fig. 3, if there is no energy barrier between the two configurations. Moreover, the flips of vacancy relaxation pattern require the application of quite noticeable strains (>2%), so the energy barriers are in any case non-negligible. Hence, the co-existence of several metastable configurations should reflect a real physical effect. In other words, we can consider the vacancy in silicon as a multi-symmetry defect, in the sense that, except for cryogenic temperatures, different stable vacancy configurations coexist in silicon crystals.

In addition to monovacancies, we have studied the atomic and electronic structure of two complexes of a vacancy with a donor atom (As or Sb). Both complexes (AsV and SbV) were studied in four different charge states, from +1 to –2.

As seen in Table 3, the relaxation patterns of both E-centers are qualitatively very similar, but the degree of relaxation is notably different. The vacancy nearest-neighbors in the AsV complex manifest more pronounced inward relaxation than in SbV (the difference in relaxation volumes is about 4%). This is due most probably to the different atomic sizes of As and Sb incorporated into the silicon lat-

tice. Indeed, according to our calculations, a substitutional As atom induces a small (~3%) inward relaxation of the nearest-neighbor shell, whereas Sb atom forces an outward relaxation (by 6.5%).

For both complexes, two bonding types, namely PB and RB, were found to be stable in all considered charge states. In addition, breathing relaxation mode was also found to be stable for charge states +1 and –1 of AsV, while the doubly negatively charged AsV exhibited a special kind of bonding structure—resonant split. Resonant split configuration is formed when As or Sb atom shifts towards the midpoint between its own site and the vacant one. In a sense, the vacancy is split into two half-vacancies, so that the triangle of atoms nearest to As in one half-vacancy interacts via resonant bonding (RB), whereas that in another one—via pairing bonding (PB).

Similar to the monovacancy case, the energy of the E-center in a fixed charge state is weakly sensitive to the bonding mode, varying within 0.1 eV for different complex configurations. It can therefore be concluded that a flat interatomic interaction potential surface with a number of shallow local minima seems to be a fundamental property of the vacancy-type defects in silicon.

The existence of different relaxation mode patterns is manifested in the different band structures of crystals with E-centers. In order to demonstrate it, we have calculated the band structures for two different relaxation patterns (RB and PB) of AsV, Fig. 4. These two modes result in notably different band structures for AsV, with the middle defect level shifting downwards in PB. From the experimental point of view, this result means that the possible co-existence of E-centers with various symmetries should be taken into account during the identification of the defect. Unfortunately, such measurable parameters as defect ionization levels cannot be used to probe the relaxation patterns of E-centers. Indeed, the defect formation energies in the different relaxation modes are nearly the same and so the ionization levels are practically insensitive to the existence of multiple complex symmetries.

4. Summary

Summing up, we have demonstrated that vacancy-based defects in silicon can coexist in several metastable configurations with very similar formation energies in all possible charge states. In other words, vacancy-type defects in silicon can be considered as multi-symmetry defects in the sense that, even at relatively low temperatures, the probabilities to find vacancies in different stable configurations remain comparable. At elevated temperatures, the relaxation pattern around the same defect can easily switch between different metastable configurations and dwell in them for comparable times.

Table 3

Formation energies and bonding modes for AsV and SbV (RB=resonant bond; PB=pairing bond; BM=breathing mode; S=split). E-center charges are indicated in column headers.

	Formation energy (eV)/bonding type			
	+1	0	–1	–2
AsV	2.24 RB/PB/BM	2.31 RB/PB	2.42 RB/PB/BM/S	2.98 RB/PB/S
SbV	9.78 RB/PB	9.93 RB/PB	10.26 RB/PB	10.73 RB/PB/S

Acknowledgements

The work was supported by the Academy of Finland through the Centers of Excellence program (2006–2011) and by the grant #08-08-90012 from the Russian Foundation for Basic Research. We also wish to thank the Center for Scientific Computing (Helsinki, Finland) for the use of their computational facilities.

References

- [1] D.J. Paul, *Phys. World* 13 (2000) 27.
- [2] M.J. Puska, S. Pöykkö, M. Pesola, R.M. Nieminen, *Phys. Rev. B* 58 (1998) 1318.
- [3] O.K. Al-Mushadani, R.J. Needs, *Phys. Rev. B* 68 (2003) 235205.
- [4] H. Seong, L.J. Lewis, *Phys. Rev. B* 53 (1996) 9791.
- [5] P.J. Kelly, R. Car, *Phys. Rev. B* 45 (1992) 6543.
- [6] M.G. Ganchenkova, A. Nazarov, A. Kuznetsov, *Nucl. Instrum. Meth. Phys. Res. B* 202 (2003) 107.
- [7] A. Antonelli, J. Bernholc, *Phys. Rev. B* 40 (1989) 10643.
- [8] A. Nylandsted Larsen, A. Mesli, K. Bonde Nielsen, H. Kortegaard Nielsen, L. Dobaczewski, J. Adey, R. Jones, D.W. Palmer, P.R. Briddon, S. Öberg, *Phys. Rev. Lett.* 97 (2006) 106402.
- [9] F. d'Acapito, S. Milita, A. Satta, L. Colombo, *J. Appl. Phys.* 102 (2007) 043524.
- [10] H. Bracht, E.E. Haller, R. Clark-Phelps, *Phys. Rev. B* 52 (1995) 16542.
- [11] H. Bracht, E.E. Haller, R. Clark-Phelps, *Phys. Rev. Lett.* 81 (1998) 393.
- [12] H. Bracht, J.F. Pedersen, N. Zangenberg, A. Nylandsted Larsen, E.E. Haller, G. Lulli, M. Posselt, *Phys. Rev. Lett.* 91 (2003) 245502.
- [13] V. Ranki, K. Saarinen, *Phys. Rev. Lett.* 93 (2004) 255502.
- [14] G.D. Watkins, J.W. Corbett, *Phys. Rev.* 134 (1964) A1359.
- [15] S. Dannefaer, P. Mascher, D. Kerr, *Phys. Rev. Lett.* 56 (1986) 2195.
- [16] G.D. Watkins, *J. Appl. Phys.* 103 (2008) 106106.
- [17] A.O. Evwaraye, E. Sun, *J. Appl. Phys.* 47 (1976) 3776.
- [18] G.D. Watkins, in: S.T. Pantelides (Ed.), *Deep Centers in Semiconductors*, Gordon and Breach, New York, 1986, p. 147.
- [19] Y. Shimizu, M. Uematsu, K.M. Itoh, *Phys. Rev. Lett.* 98 (2007) 095901.
- [20] G.D. Watkins, *J. Phys. Soc. Jpn.* 18 (Suppl. II) (1963) 22.
- [21] G.D. Watkins, J.R. Troxell, A.P. Chatterjee, *Inst. Phys. Conf. Ser.* 46 (1979) 18.
- [22] E. Tarnow, *J. Phys. Condensed Matter* 5 (1993) 1863.
- [23] A. Zyweitz, J. Furthmüller, F. Bechstedt, *Mater. Sci. Forum* 258–268 (1997) 653.
- [24] G.D. Watkins, *Physica* 117B–118B (1983) 9.
- [25] G.A. Baraff, E.O. Kane, M. Schlüter, *Phys. Rev. B* 21 (1980) 5662.
- [26] G.D. Watkins, J.R. Troxell, *Phys. Rev. Lett.* 44 (1980) 593.
- [27] C.D. Latham, M.G. Ganchenkova, R.M. Nieminen, S. Nicolaysen, M. Alatalo, S. Öberg, P.R. Briddon, *Phys. Scr.* T126 (2006) 61.
- [28] E.L. Elkin, G.D. Watkins, *Phys. Rev.* 174 (1968) 881.
- [29] G.D. Watkins, *Radiat. Effects Def. Solids* 111–112 (1989) 487.
- [30] S. Ögüt, J. Chelikowsky, *Phys. Rev. Lett.* 91 (2003) 235503.
- [31] M.G. Ganchenkova, A.Yu. Kuznetsov, R.M. Nieminen, *Phys. Rev. B* 70 (2004) 1.
- [32] A.F. Wright, *Phys. Rev. B* 74 (2006) 165116.
- [33] J.P. Perdew, J.A. Chevary, S.H. Vosko, K.A. Jackson, M.R. Pederson, D.J. Singh, C. Fiolhais, *Phys. Rev. B* 46 (1992) 6671.
- [34] G. Kresse, J. Furthmüller, *Comp. Mater. Sci.* 6 (1996) 15.
- [35] G. Kresse, J. Furthmüller, *Phys. Rev. B* 54 (1996) 11169.
- [36] W. Kohn, L.J. Sham, *Phys. Rev.* 140 (1965) A1133.
- [37] D. Vanderbilt, *Phys. Rev. B* 41 (1990) 7892.
- [38] H.J. Monkhorst, J.D. Pack, *Phys. Rev. B* 13 (1976) 5188.
- [39] J.W. Corbett, J.C. Bourgoin, in: J.H. Crawford Jr., L.M. Slifkin (Eds.), *Semiconductors and Molecular Crystals*, vol. 2, Plenum Press, New York, 1975.